Catal Lett (2008) 123:321–326
DOI 10.1007/s10562-008-9426-4

Effect of CeO_2 Doping on Structure and Catalytic Performance of Co_3O_4 Catalyst for Low-Temperature CO Oxidation

Xiao-Dong Hou · Yong-Zhao Wang · Yong-Xiang Zhao

Received: 16 December 2007 / Accepted: 4 February 2008 / Published online: 16 February 2008

Abstract The effect of CeO_2 doping on structure and catalytic performance of Co_3O_4 catalyst was studied for low-temperature CO oxidation. The Co_3O_4 catalyst was prepared by a precipitation method and the CeO_2/Co_3O_4 catalyst was prepared by an impregnation method. Their catalytic performance had been studied with a continuous flowing microreactor. The results reveal that the CeO_2/Co_3O_4 catalyst exhibits much better resistance to water vapor poisoning than the Co_3O_4 catalyst for CO oxidation. The CeO_2/Co_3O_4 catalyst can maintain CO complete conversion at least 8,400 min at 110 °C with 0.6% water vapor in the feed gas, while the Co_3O_4 catalyst can maintain at 100% for only 100 min. Characterizations with XRD, TEM and TPR suggest that the CeO_2/Co_3O_4 catalyst possesses higher dispersion degree, smaller particles and larger S_{BET}, due to the doping of Ceria, and exists the interaction between CeO_2 and Co_3O_4, which may contribute to the excellent water resistance for low-temperature CO oxidation. Furthermore, the H_2 detected in the reactor outlet gas seems to indicate that the water–gas shift reaction is the more direct reason.

Keywords Co_3O_4 · CeO_2/Co_3O_4 · Carbon monoxide oxidation · Water resistance

1 Introduction

The low-temperature catalytic oxidation of CO has become an important research topic over the years due to its many potential fields of applications [1–4]. Precious metal catalysts, such as Pd-based catalysts [5, 6] and Au-based catalysts [7, 8] have been studied and show high catalytic activities for CO oxidation. However, the sensitivity of precious metals to sulfur poisoning and their high cost have long motivated the search for substitute catalysts including various transition metal oxides [9–17].

As a promising candidate of precious metal catalysts, cobalt oxide catalysts have attracted considerable attentions because of not only its high activity for CO and hydrocarbon oxidation [18, 19], but also its use in the Fischer–Tropsch synthesis [20], NO decomposition [21], and ammonia oxidation [22]. The low-temperature CO oxidation over single component, composite and supported cobalt oxide catalysts have been studied [12–18], and these cobalt oxides show significant catalytic activity for CO oxidation. However, if water vapor exists in the feed gas, the catalytic activity of cobalt oxide catalysts decreases rapidly [23], which limits the application of the catalyst in many fields.

Ceria has a high oxygen storage capacity and well-known catalytic and redox properties (couples of Ce^{4+}/Ce^{3+}), making more oxygen available for the oxidation process [24]. Besides being widely used in the automotive three-way catalytic converter [25] and participating directly in chemical process [26], it improves CO oxidation [9, 27].

Due to the sensitivity of the cobalt oxide catalysts to water vapor and the advantages of ceria, the oxidation of CO over CoO_x/CeO_2 have been studied [27, 28]. Kang min et al. [27] prepared the CoO_x/CeO_2 catalyst by a co-precipitation method and found that it exhibited excellent water resistance for CO oxidation at 150 °C. Shao et al. [28] found that the CoO_x/CeO_2 catalyst, prepared by a co-precipitation–oxidation method, also had a very good

X.-D. Hou · Y.-Z. Wang · Y.-X. Zhao (✉)
Engineering Research Center of Fine Chemicals Ministry of Education, School of Chemistry and Chemical Engineering, Shanxi University, Taiyuan 030006, China
e-mail: yxzhao@sxu.edu.cn

water resistance. They attributed mainly the excellent water resistance to the interaction between CeO_2 and Co_3O_4 in the Co_3O_4/CeO_2 catalyst.

In our previous work [18], the single component Co_3O_4 catalyst with high activity and stability had been developed with a very simple preparation method. In the present work, the CeO_2/Co_3O_4 catalyst with excellent water resistance had been prepared for CO oxidation. The effect of CeO_2 doping on structure and catalytic performance of Co_3O_4 catalyst was studied for low-temperature CO oxidation. Combined with characterizations, a possible reason for the excellent water resistance of the CeO_2/Co_3O_4 catalyst has been given.

2 Experimental

2.1 Catalyst Preparation

The Co_3O_4 samples were prepared via a liquid-precipitation method in an aqueous solution and calcined at 300 and 400 °C for 3 h, respectively. The detailed preparation procedure was described in our previous paper [18].

The CeO_2/Co_3O_4 catalyst was prepared by impregnation of the Co_3O_4 calcined at 300 °C with an aqueous solution of desired concentration of $Ce(NO_3)_3{\cdot}6H_2O$ (the ceria loading is 5 wt%) , drying at 110 °C for 24 h, and calcination in air at 400 °C for 3 h. The Co_3O_4 catalyst calcined at 400 °C was used for comparison. Pure CeO_2 was prepared by decomposition of $Ce(NO_3)_3{\cdot}6H_2O$ at 400 °C for 3 h in air.

2.2 Catalyst Characterization

X-ray diffraction (XRD) measurements were performed using a Rigaku D/MAX-2250 X-ray diffractometer with a target of Cu K_α operated at 50 kV and 60 mA with a scanning speed of 0.5°/min and a scanning angle (2θ) range of 10–80°. Average particle size of the samples was evaluated from X-ray line broadening analysis (XLBA) using the well-known Scherer equation ($d = 0.89\lambda/\beta\cos\theta$) [29].

N_2 adsorption–desorption isotherms at −196 °C were determined using Micrometritics ASAP 2020 special surface area and porosity analyzer. Prior to the sorption experiments, the samples were degassed under vacuum at 150 °C for 12 h. The specific surface area (S_{BET}) was determined from the nitrogen adsorption isotherm.

Transmission electron microscopy (TEM) measurements were carried out using Hitachi H-600-2 TEM operated at 75 kV. Samples for TEM were dispersed by ultrasonic in acetone followed by deposition of the suspension onto a standard Cu grid covered with a holey carbon film.

Temperature-programmed reduction (TPR) provided information about catalyst reducibility. Five percent H_2/N_2 flow passed through 30 mg of catalyst with a flow rate of 20 ml min^{-1}. The temperature was ramped from room temperature to 800 °C at 10 °C min^{-1}.

Fourier transform infrared spectra (FT-IR) of the samples were obtained on a Bruker TENSOR 27 spectrometer in the range of 400–800 cm^{-1}. One milligram of each powder sample was diluted with 200 mg of potassium bromide (KBr) powder.

2.3 Apparatus and Method for Activity Test

The measurements of catalytic performance for low-temperature CO oxidation were carried out in a continuous flow laboratory microreactor under atmospheric pressure. The microreactor was 8 mm i.d. quartz u-tube, and a thermocouple was set into the catalyst bed to measure the temperature. The samples were sieved to 40–60 mesh so that concentration and temperature gradients as well as pressure drop over the catalyst bed were negligible. About 300 mg of catalysts was used for each run. The feed gas was adjusted by mass flow controllers consisted of 0.5vol% CO, 14.4 vol% O_2 and 85.1 vol % N_2, passed through the catalyst bed with a total flow rate of 20 ml min^{-1}. The feed gas in water vapor condition was obtained by passing the mixed gas through a water bubbler. The variety of water vapor content was realized by adjusting the temperature of the water bubbler. Quantitative analysis of CO and CO_2 was performed with an on-line gas chromatograph equipped with a 3 m column packed with carbon molecular sieve, a methanator and a Flame Ionization Detector (FID). In order to enhance the sensitivity of the detection, CO and CO_2 were converted to CH_4 by the mathenator at 360 °C before entering into the FID. The minimum detection level was ca. 10 ppm. In addition, the reactor outlet gas was also analyzed qualitatively using thermal conductivity detector (TCD). Prior to all catalytic experiments the catalysts were pretreated in flowing air at 200 °C for 30 min to yield clean surface and then cooled in the absence of flowing air.

3 Results and Discussion

3.1 Characterization of Catalysts

The XRD patterns of the Co_3O_4 and CeO_2/Co_3O_4 catalysts are shown in Fig. 1. Characteristic spinel Co_3O_4 peaks are detected in the both catalysts. But CeO_2 peaks are not observed in the CeO_2/Co_3O_4 catalyst, meaning that the CeO_2 exists in the catalyst as a high dispersed state. From the Fig. 1, the characteristic spinel Co_3O_4 peaks broaden

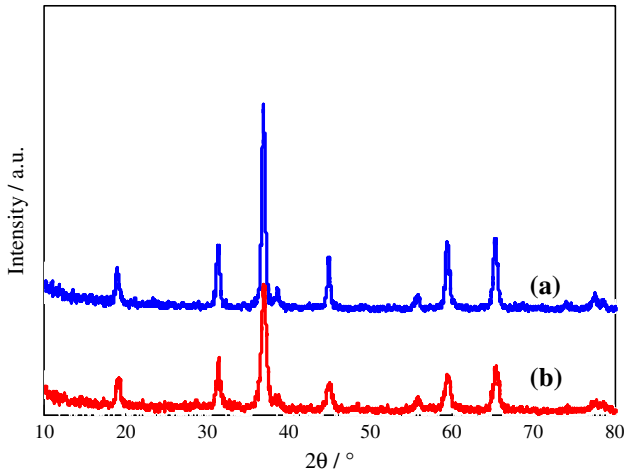

Fig. 1 XRD patterns of the Co_3O_4 and CeO_2/Co_3O_4 catalysts: (**a**) Co_3O_4; (**b**) CeO_2/Co_3O_4

due to the doping of a small quantity of ceria. The average particle size of the Co_3O_4 and CeO_2/Co_3O_4 catalysts is 18 and 10 nm, respectively, calculated using the Scherer equation. Apparently, the Co_3O_4 in the composite catalyst has a higher dispersion degree and the doping of a small quantity of ceria can significantly increases the thermal stability of the Co_3O_4 species in the CeO_2/Co_3O_4 catalyst. The S_{BET} of the Co_3O_4 and CeO_2/Co_3O_4 catalysts is 46 and 70 $m^2\ g^{-1}$, respectively determined from nitrogen adsorption isotherms. Increasing of the S_{BET} of the CeO_2/Co_3O_4 catalyst is attributed possibly to the higher dispersion degree of Co_3O_4 in the composite catalyst due to the doping of a small quantity of Ceria, which is generally consistent with our TEM observation (will be presented shortly).

It is clear that the TEM image (b) of the CeO_2/Co_3O_4 catalyst shows monodisperse and ultrafine particles in the Fig. 2. But the significant aggregation of the Co_3O_4 catalyst can be observed from the TEM image (a) and may induce the decrease of the S_{BET} of the Co_3O_4 catalyst. The particle size of the Co_3O_4 and CeO_2/Co_3O_4 catalysts estimated from TEM is 20–25 and 10–15 nm, respectively, which is generally consistent with the calculation from the broadening of powder diffraction peaks in X-ray patterns. Apparently, the CeO_2/Co_3O_4 catalyst shows good sintering resistance due to the doping of CeO_2.

Figure 3 shows the TPR profiles of various catalysts. The Co_3O_4 and CeO_2/Co_3O_4 catalysts include two reduction peaks, namely α peak and β peak. According to the literature [21], the low-temperature α peak ($P_{H_2} - \alpha$) can be ascribed to the reduction of Co^{3+} ions, present in the spinel structure, into Co^{2+}, with the subsequent structure change to CoO, which follows the higher-temperature β peak ($P_{H_2} - \beta$) and is due to the reduction of CoO to metallic cobalt. The peaks can be attributed to the step-wise reduction of cobalt oxide via $Co^{3+} \rightarrow Co^{2+} \rightarrow Co^0$. There are two H_2 consumption peaks in the TPR profile of CeO_2 in the Fig. 3. The peak at around 530 °C ($P_{H_2} - \gamma$) is due to the reduction of surface oxygen species. The higher temperature peak ($P_{H_2} - \delta$) appeared at around 840 °C is attributed to the bulk reduction of CeO_2 by elimination of O^{2-} anions of the lattice and formation of Ce_2O_3 [30]. From the Fig. 3, the doping of a small quantity of Ceria makes the reduction peak of Co_3O_4 in the CeO_2/Co_3O_4 catalyst shift to higher temperature, which is in accord with the literature [12]. In addition, the peak area ratio of $P_{H_2} - \beta / P_{H_2} - \alpha$ for the Co_3O_4 catalyst is 3.01:1, which is quantitatively consistent with the theoretical calculation.

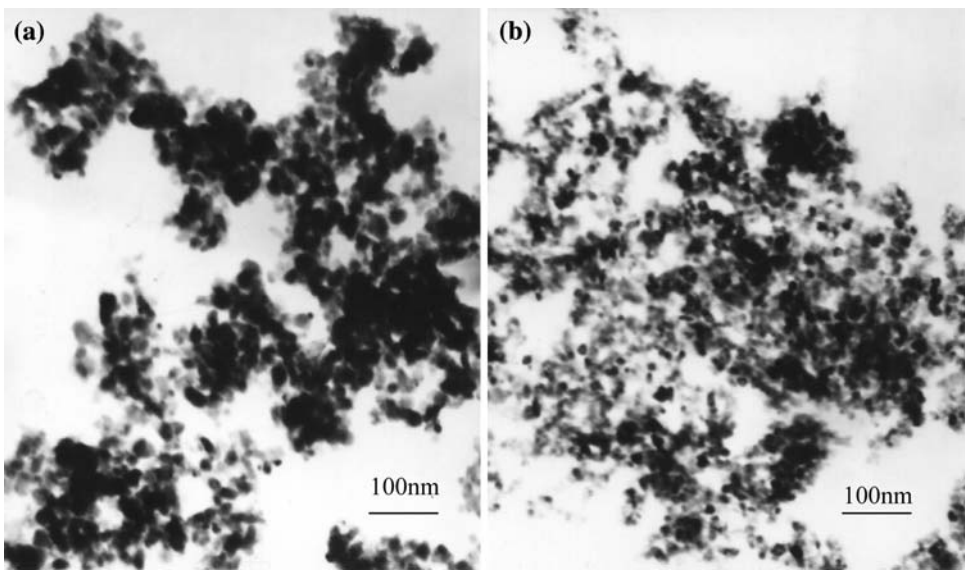

Fig. 2 TEM images of the Co_3O_4 and CeO_2/Co_3O_4 catalysts: (**a**) Co_3O_4; (**b**) CeO_2/Co_3O_4

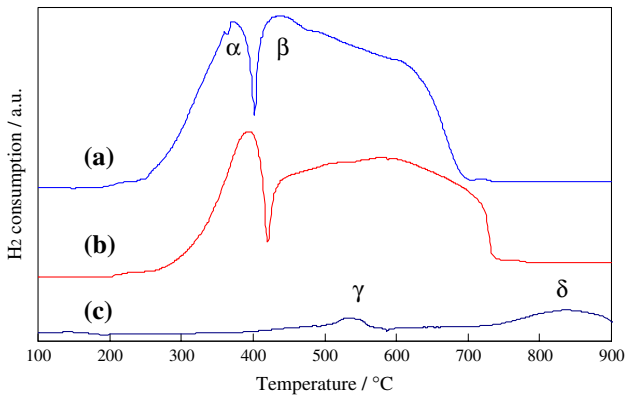

Fig. 3 TPR profiles of various catalysts: (a) Co_3O_4; (b) CeO_2/Co_3O_4; (c) CeO_2

But it is 4.29:1 for the CeO_2/Co_3O_4 catalyst. If the β peak of the CeO_2/Co_3O_4 catalyst is ascribed to the reduction of Co^{2+} to Co^0 only, this result would mean that there are more Co^{2+} in the CeO_2/Co_3O_4 catalyst than in pure Co_3O_4. However, we have not detected the presence of more Co^{2+} (in the form of CoO) in the XRD. Therefore, there must be some other reduction reaction occurred that corresponds to this peak. One may notice the presence of H_2 consumption peaks of ceria ($P_{H_2} - \gamma$ and $P_{H_2} - \delta$). Although these peaks were very weak for pure ceria, their contribution to $P_{H_2} - \beta$ of CeO_2/Co_3O_4 could be enhanced by the presence of cobalt. According to the literatures [30, 31], the easier reduction of Ceria in the presence of transition metal is generally interpreted as a spill-over process of the metal to Ceria. Since the reduction of Co^{2+} to Co occurs at the temperature of β peak, the formation of Co may enable hydrogen to reduce CeO_2. So the reduction of CeO_2 also contributes to the β peak. According to the result of TPR, there is the significant interaction between CeO_2 and Co_3O_4 in the CeO_2/Co_3O_4 catalyst.

Figure 4 shows the FT-IR spectra of the Co_3O_4 and CeO_2/Co_3O_4 catalysts. Both of the samples show two distinctive bands at ca. 567 (v_1) and 665 cm^{-1} (v_2), originating from the stretching vibrations of the cobalt–oxygen bond of Co_3O_4 spinel oxide [12, 16]. The v_1 band is associated with OB_3 vibrations in the spinel lattice, where B denotes the Co^{3+} in an octahedral position, and the v_2 band is attributed to the ABO_3 vibrations, where A denotes the Co^{2+} in a tetrahedral position [18]. The v_1 band of Co_3O_4 in the CeO_2/Co_3O_4 catalyst shifts slightly to higher wavenumber, compared to that of the single component Co_3O_4 catalyst, meaning the existence of the interaction between CeO_2 and Co_3O_4 in the composite catalyst.

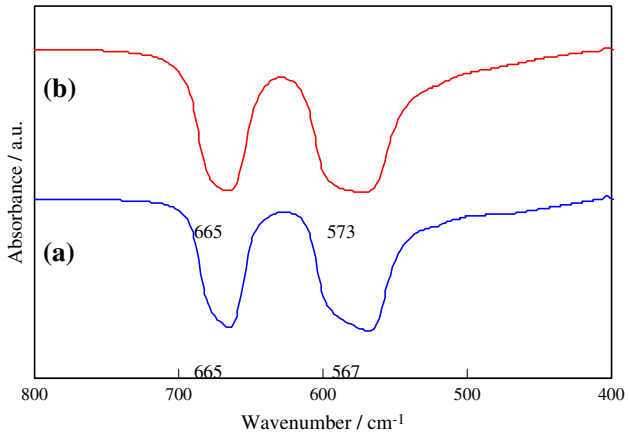

Fig. 4 IR characterization of the Co_3O_4 and CeO_2/Co_3O_4 catalysts: (a) Co_3O_4; (b) CeO_2/Co_3O_4

3.2 Catalytic Performance for Low-Temperature CO Oxidation

Figure 5 illustrates the stability of various catalysts for CO oxidation with 0.6% water vapor in the feed gas at room temperature. As seen from the Fig. 5, CO complete conversion over the Co_3O_4 and CeO_2/Co_3O_4 catalysts could be maintained for only 20 min. So the both catalysts are very sensitive to water vapor in the feed gas at room temperature. When the reaction temperature is raised to 110 °C (seeing the Fig. 6), CO complete conversion is maintained at least 8,400 min over the CeO_2/Co_3O_4 catalyst with 0.6% water vapor in the feed gas. However, the CO complete conversion can be maintained for only 100 min over the Co_3O_4 catalyst under the same condition. In addition, seeing from the Fig. 6, the CO complete conversion over the physically mixed $CeO_2-Co_3O_4$ catalyst (5 wt% CeO_2) can be maintained for only 130 min which is close to the catalytic performance of the single component Co_3O_4 catalyst. At room temperature, pure CeO_2 has an original conversion of 4.1%, but deactivates rapidly for CO oxidation with 0.6% water vapor in the feed gas (seeing the Fig. 5). When the reaction temperature is raised to 110 °C, the conversion increases to 6.5%, then gradually decreases to 2.9% within 120 min over pure CeO_2 (seeing the Fig. 6).

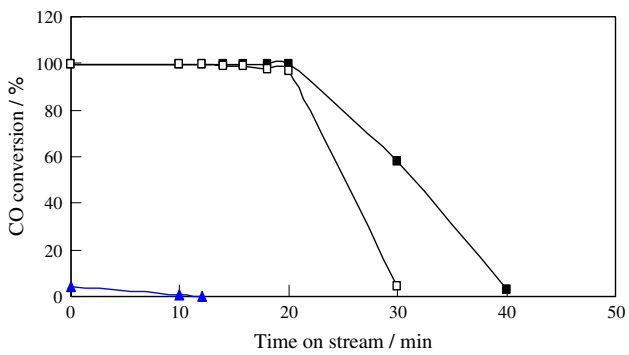

Fig. 5 Catalytic performance of various catalysts in the presence of 0.6% water vapor in the feed gas at room temperature: ■ CeO_2/Co_3O_4; □ Co_3O_4; ▲ pure CeO_2

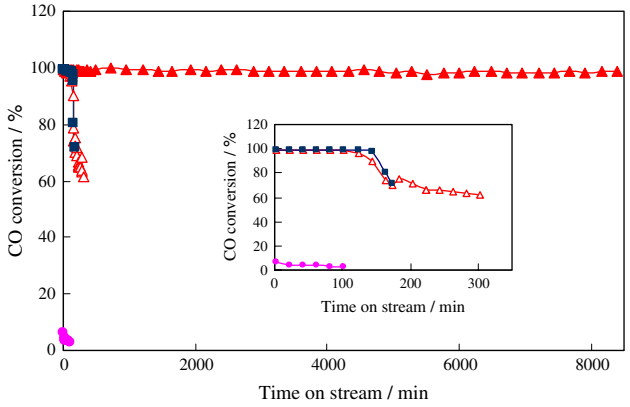

Fig. 6 Catalytic performance of various catalyst in the presence of 0.6% water vapor in the feed gas at 110 °C: ▲ CeO_2/Co_3O_4; △ Co_3O_4; ■ physically mixed CeO_2–Co_3O_4; ● pure CeO_2 Inset: The inset shows a magnification of the left curves for a clear comparison

Apparently, the water resistance of the CeO_2/Co_3O_4 catalyst is much better than the single component Co_3O_4 and physically mixed catalysts for low-temperature CO oxidation. Pure CeO_2 has a very low activity for CO oxidation at both room temperature and 110 °C. This illuminates that there is a synergistic effect between Co_3O_4 and CeO_2, which strongly affect the water resistance of the CeO_2/Co_3O_4 catalyst for CO oxidation. According to the characterization results, the CeO_2/Co_3O_4 catalyst possesses higher dispersion degree, smaller particles and larger S_{BET} than the single component Co_3O_4 catalyst due to the doping of a small quantity of Ceria. In addition, Ceria has a high oxygen storage capacity and well-known redox properties, and the activity of catalysts to water–gas shift reaction (WGSR) is improved by the addition of Ceria [32–34]. Moreover, a trace quantity of H_2 is detected by TCD in the reactor outlet gas in the CO oxidation reaction. But, the H_2 is not detected in the reactor outlet gas for the single component Co_3O_4 catalyst. Thus we can conclude that water–gas shift reaction occurs over the CeO_2/Co_3O_4 catalyst in the CO oxidation reaction at 110 °C. The WGSR between adsorbed CO and the hydroxyl groups on ceria may proceed through the redox mechanism.

$$CO(ads) + 2CeO_2 = CO_2 + Ce_2O_3,$$

$$OH + Ce_2O_3 = 2CeO_2 + 1/2\ H_2$$

where CeO_2 is reduced to Ce_2O_3 by CO to give CO_2 and the hydroxyl group then react with Ce_2O_3 to give CeO_2 and H_2 [35]. H_2O molecules are competitively absorbed to the active sites and poison the cobalt oxide surface [23], which makes the single component Co_3O_4 catalyst deactivate within a period of time. But, with the doping of CeO_2, H_2O absorbed on the composite catalyst can be decomposed via WGSR. Thus, CO can be completely converted for a long time in the water vapor condition. So we think the water–gas shift reaction is the more direct reason for the excellent water resistance of the CeO_2/Co_3O_4 catalyst for low-temperature CO oxidation.

The catalytic stability of the CeO_2/Co_3O_4 catalyst was further investigated at various temperatures. After CO complete oxidation was maintained for 8,400 min over the CeO_2/Co_3O_4 catalyst, the reaction temperature decreased from 110 to 100 °C and the water vapor content was kept to 0.6%. As seen from the Table 1, the CO conversion decreases to 87.9% after the temperature maintains at 100 °C for 60 min. Then the reaction temperature ramps from 100 to 110 °C at 1 °C/min. The CO conversion is able to return to 100% after the temperature maintains at 110 °C for 240 min.

The effect of water vapor content on water resistance of the CeO_2/Co_3O_4 catalyst for CO oxidation was also studied at 110 °C showing in the Table 2. CO conversion over the composite catalyst is 97.3% after maintaining the water vapor content at 1.8% for 4,220 min. But CO conversion decreases to 94.4% when water vapor content rises to 4.0% and passes for 240 min. However, CO conversion can return again to 100% after 60 min when the water vapor content returns to 0.6%. From the Tables 1 and 2, one can

Table 1 The effect of reaction temperature on water resistance of the CeO_2/Co_3O_4 catalyst

Reaction temperature (°C)	Sustaining time[a] (min)	CO conversion[b] (%)
105		98.1
100	30	90.8
	60	87.9
110	30	98.1
	60	97.8
	240	100

[a] Sustaining time at the certain temperature

[b] CO conversion tested after corresponding time maintained at the certain temperature

Table 2 The effect of water vapor content on water resistance of the CeO_2/Co_3O_4 catalyst

Water vapor content (%)	Time[a] (min)	CO conversion[b] (%)
1.8	4,220	97.3
4.0	30	97.0
	60	95.7
	120	94.5
	240	94.4

[a] Keeping time at the certain water vapor content

[b] CO conversion tested after corresponding time maintained at the certain water vapor content

be suggested that the CeO_2/Co_3O_4 catalyst is very sensitive to the reaction temperature and the water vapor content in the feed gas, but the deactivation is reversible.

4 Conclusions

The CeO_2/Co_3O_4 catalyst was prepared with a simple precipitation–impregnation method and the effect of CeO_2 doping on the structure and catalytic performance of Co_3O_4 catalyst had been investigated. The tests for CO oxidation indicate that at room temperature, the Co_3O_4 and CeO_2/Co_3O_4 catalysts are both very sensitive to water vapor in the feed gas and they can maintain CO complete conversion for only 20 min with 0.6% water vapor. Surprisingly, when the reaction temperature rises to 110 °C, CO complete oxidation over the CeO_2/Co_3O_4 catalyst can be maintained at least 8,400 min, showing very good water resistance. But the CO complete oxidation can be maintained for only 100 min over the Co_3O_4 catalyst. The characteristic results reveal that the CeO_2/Co_3O_4 catalyst possesses higher dispersion degree, smaller particle and larger surface area, due to the doping of a small quantity of CeO_2, and exists the interaction between CeO_2 and Co_3O_4, which may contributed to the excellent resistance to water vapor poisoning for CO oxidation over the composite catalyst. Furthermore, the H_2 detected in the reactor outlet gas seems to indicate that the water–gas shift reaction is the more direct reason.

Acknowledgments The authors thank the Shanxi Natural Science Foundation (grants: 20041017) and Shanxi Scientific & Technological Promoted Project of China (grants: 031099) for the financial support of this work.

References

1. Yamaura H, Moriya K, Miura N, Yamazoe N (2000) Sens Actuators B 65:39
2. Thormählen P, Fridell E, Cruise N, Skoglundh M, Palmqvist A (2001) Appl Catal B 31:1
3. Shelef M, McCabe RW (2000) Catal Today 62:35
4. Kim DH, Lim MS (2002) Appl Catal A 224:27
5. Dong GL, Wang JG, Gao YB, Chen SY (1999) Catal Lett 58:37
6. Margitfalvi JL, Borbáth I, Hegedűs M, Tfirst E, Gőbölös S, Lázár K (2000) J Catal 196:200
7. Jia ML, Shen YN, Li CY, Bao ZRGT, Sheng SS (2005) Catal Lett 99:235
8. Chiang CW, Wang AQ, Wan BZ, Mou CY (2005) J Phys Chem B 109:18042
9. Liu W, Flytzani-Stephanopoulos M (1995) J Catal 153:304
10. Hutchings GJ, Mirzaei AA, Joyner RW, Siddiqui MRH, Taylor SH (1998) Appl Catal A 166:143
11. Bae CM, Ko JB, Kim DH (2005) Catal Commun 6:507
12. Jia MJ, Zhang WX, Tao YG, Wang GY, Cui XH, Zhang CL, Wu TH (1999) Chem J Chin Univ 20:637 (in Chinese)
13. Lin HK, Chiu HC, Tsai HC, Chien SH, Wang CB (2003) Catal Lett 88:169
14. Tang CW, Kuo CC, Kuo MC, Wang CB, Chien SH (2006) Appl Catal A 309:37
15. Cunningham DAH, Kobayashi T, Kamijo N, Haruta M (1994) Catal Lett 25:257
16. Jansson J (2000) J Catal 194:55
17. Thormählen P, Skoglundh M, Fridell E, Andersson B (1999) J Catal 188:300
18. Wang YZ, Zhao YX, Gao CG, Liu DS (2007) Catal Lett 116:136
19. Drago RS, Jurczyk K, Singh DJ, Young V (1995) Appl Catal B 6:155
20. Steen EV, Schulz H (1999) Appl Catal A 186:309
21. Zhang ZL, Geng HR, Zheng LS, Du B (2005) J Alloys Compd 392:317
22. Schmidt-Szaowski K, Krawczyk K, Petryk J (1998) Appl Catal A 175:147
23. Grillo F, Natile MM, Glisenti A (2004) Appl Catal B 48:267
24. Martinez-Arias A, Fernandez-Garcia M, Galbez O, Coronada JM, Anderson JA, Conesa JC, Soria J, Munuera G (2000) J Catal 195:207
25. Terribile D, Trovarelli A, Llorca J, Leitenburg CD, Dolcetti G (1998) Catal Today 43:79
26. Meunier FC, Reida D, Goguet A, Shekhtman S, Hardacre C, Burch R, Deng W, Flytzani-Stephanopoulos M (2007) J Catal 247:277
27. Kang M, Song MW, Lee CH (2003) Appl Catal A 251:143
28. Shao JJ, Zhang P, Tang XF, Zhang BC, Liu JL, Xu YD, Shen WJ (2006) Chin J Catal 27:937
29. Langford JI, Wilson AJC (1978) J Appl Crystallogr 11:102
30. Li X, Zhang C, He H, Teraoka Y (2007) Appl Catal B 75:167
31. Ernst B, Hilaire L, Kennemann A (1999) Catal Today 50:413
32. Hilaire S, Wang X, Luo T, Gorte RJ, Wagner J (2001) Appl Catal A 215:271
33. Bunluesin T, Gorte RJ, Graham GW (1998) Appl Catal B 15:107
34. Tabakova T, Idakiev V, Papavasiliou J, Avgouropoulos G, Ioannides T (2007) Catal Commun 8:101
35. Zhu HQ, Qin ZF, Shan WJ, Shen WJ, Wang JG (2004) J Catal 225:267